HHS Public Access

Author manuscript

Biomaterials. Author manuscript; available in PMC 2023 February 01.

Published in final edited form as:

Biomaterials. 2021 September ; 276: 121032. doi:10.1016/j.biomaterials.2021.121032.

A robust vasculogenic microfluidic model using human immortalized endothelial cells and Thy1 positive fibroblasts

Zhengpeng Wan[a,b,1], **Shun Zhang**[a,1], **Amy X. Zhong**[a], **Sarah E. Shelton**[a,b], **Marco Campisi**[b,c], **Shriram K. Sundararaman**[b], **Giovanni S. Offeddu**[a], **Eunkyung Ko**[d], **Lina Ibrahim**[d], **Mark F. Coughlin**[a], **Tiankun Liu**[a,e], **Jing Bai**[a], **David A. Barbie**[b,**], **Roger D. Kamm**[a,d,*]

[a]Department of Biological Engineering, Massachusetts Institute of Technology, Cambridge, MA, 02139, USA

[b]Department of Medical Oncology, Dana-Farber Cancer Institute, Boston, MA, 02215, USA

[c]Department of Mechanical and Aerospace Engineering, Politecnico di Torino, Turin, 10129, Italy

[d]Department of Mechanical Engineering, Massachusetts Institute of Technology, Cambridge, MA, 02139, USA

[e]Biomanufacturing Center, Department of Mechanical Engineering, Tsinghua University, Beijing, 100084, China

Abstract

Human umbilical vein endothelial cells (HUVECs) and stromal cells, such as human lung fibroblasts (FBs), have been widely used to generate functional microvascular networks (μVNs) *in vitro*. However, primary cells derived from different donors have batch-to-batch variations and limited lifespans when cultured *in vitro*, which hampers the reproducibility of μVN formation. Here, we immortalize HUVECs and FBs by exogenously expressing human telomerase reverse transcriptase (hTERT) to obtain stable endothelial cell and FB sources for μVN formation *in vitro*. Interestingly, we find that immortalized HUVECs can only form functional μVNs with immortalized FBs from earlier passages but not from later passages. Mechanistically, we show that Thy1 expression decreases in FBs from later passages. Compared to Thy1 negative FBs, Thy1 positive FBs express higher IGFBP2, IGFBP7, and SPARC, which are important for angiogenesis and lumen formation during vasculogenesis in 3D. Moreover, Thy1 negative FBs physically block

*Corresponding author. Department of Biological Engineering, Department of Mechanical Engineering, Massachusetts Institute of Technology, Cambridge, MA, 02139, USA, rdkamm@mit.edu (R.D. Kamm). **Corresponding author. Department of Medical Oncology, Dana-Farber Cancer Institute, Boston, MA, 02215, USA, david_barbie@dfci.harvard.edu (D.A. Barbie).
[1]Indicates equal contribution of these authors.

Credit author statement

Zhengpeng Wan: Conceptualization, Methodology, Writing – original draft, Writing – review & editing. Shun Zhang: Conceptualization, Methodology, Writing – original draft, Writing – review & editing. Amy X. Zhong: Methodology, Writing – review & editing. Sarah E. Shelton: Resources, Methodology, Writing – review & editing. Marco Campisi: Methodology, Writing – review & editing. Shriram K Sundararaman: Methodology, Writing – review & editing. Giovanni S. Offeddu: Resources, Methodology, Writing – review & editing. Eunkyung Ko: Resources, Writing – review & editing. Lina Ibrahim: Writing – review & editing, Mark F. Coughlin: Writing – review & editing, Tiankun Liu: Writing – review & editing, Jing Bai: Resources, Writing – review & editing. David A. Barbie: Conceptualization, Supervision, Writing – review & editing, Funding acquisition. Roger D. Kamm: Conceptualization, Supervision, Writing – review & editing, Funding acquisition.

Appendix A. Supplementary data

Supplementary data to this article can be found online at https://doi.org/10.1016/j.biomaterials.2021.121032.

microvessel openings, reducing the perfusability of μVNs. Finally, by culturing immortalized FBs on gelatin-coated surfaces in serum-free medium, we are able to maintain the majority of Thy1 positive immortalized FBs to support perfusable μVN formation. Overall, we establish stable cell sources for μVN formation and characterize the functions of Thy1 positive and negative FBs in vasculogenesis *in vitro*.

Keywords

HUVECs; Fibroblasts; Immortalization; Vasculogenesis; Thy1; Microfluidic

1. Introduction

Generation of perfusable vasculature *in vitro* is of key importance in the development of microphysiological models of tissue or organ function and for a variety of applications in tissue engineering. This arises from the need for an adequate supply of oxygen and nutrients to tissues in order to maintain viability and function, since diffusion alone fails when cells are located more than several hundred microns from a perfusable vessel [1]. The absence of functional vasculature has posed a critical barrier to the advancement of numerous bioengineering techniques and applications. In particular, current human organoids usually lack functional vasculature, which leads to a slowly developing necrotic core [2]. Inadequate oxygen and nutrient supply further results in organoids that are small and have a limited life span, hindering the development of organoids beyond their embryonic and fetal phases [3].

Benefitting from advances in microfluidic devices, self-organized *in vitro* microvascular networks (μVNs) can now be successfully fabricated [4–6]. These designs usually involve microfluidic devices with a central gel channel flanked by two medium channels. Endothelial cells (ECs) combined with stromal cells can be suspended in a hydrogel in the gel channel. Within days, ECs will self-organize and form networks with perfusable lumens. The major advantage of the self-organizing approach is its similarity to the *in vivo* processes of vasculogenesis and angiogenesis, leading to the spontaneous formation of vessels by ECs in hydrogel mimicking *in vivo* counterparts in both form and function [7].

Most work in engineering μVNs with demonstrated perfusability is limited to primary cells such as human umbilical vein endothelial cells (HUVECs), human fibroblasts (FBs), smooth muscle cells, pericytes, astrocytes, bone marrow–derived stromal cells, and adipose-derived stem cells [4,6,8–10]. Both the diversity of donor genotypes and the limited proliferation capacity of primary cells contribute to variability in terms of the morphology and function of the resulting μVNs, leading to inconsistencies in the ability to form fully-functional μVNs [11] and a lack of reproducibility among experiments. Due to these issues, researchers have sought and applied various ways to standardize cell sources and reduce variability, including the use of immortalized cell lines. One widely utilized approach is to immortalize primary cells using human telomerase reverse transcriptase (hTERT) [12].

Thy1 is a 25–37 kDa glycosylphosphatidylinositol (GPI) anchored cell membrane protein and was first identified in 1964 on mouse T cells [13,14]. Later studies revealed that Thy1 is prevalently expressed in various cell types, including FBs, neurons, and hematopoietic cells,

and that Thy1 plays an important role in adhesion, migration, apoptosis, wound healing, tumorigenesis, fibrogenesis, and mechanosensing [15–17]. Thy1 has also been used as a marker to identify subpopulations of FBs [18]. Interestingly, previous studies have identified that Thy1 positive (Thy1+) and Thy1 negative (Thy1−) FBs derived from lung tissues have distinct functions [19,20], such as proliferation [21], differentiation to myofibroblast, and correlation with fibrosis [15,22]. However, whether the Thy1+ and Thy1− FBs have different functions in μVN formation remains unclear.

Here we demonstrate the use of hTERT to immortalize ECs and FBs with verified capability to form functional μVNs to overcome the noted limitations. Immortalized HUVECs (ImHUVECs) are shown to be a stable source for vasculogenesis, while the immortalized FBs (ImFBs) only form functional μVNs from early passages. Upon further examination, we find that lung FBs are heterogeneous for Thy1 expression, including Thy1+ and Thy1-subpopulations. The morphology of μVNs formed with Thy1+ FBs is superior to that of μVNs formed with Thy1− FBs, which we have attributed to higher expression levels of insulin-like growth factor-binding protein 2 (IGFBP2), insulin-like growth factor-binding protein 7 (IGFBP7), and secreted protein acidic and rich in cysteine (SPARC). In addition, Thy1− FBs impede perfusability by physically preventing μVNs from opening at the medium-gel interface. Finally, culturing FBs on gelatin-coated surfaces in serum-free medium can maintain most of the Thy1+ FBs, which support perfusable μVN formation. Our studies establish stable cell sources for μVN formation *in vitro* and shed light on the Thy1+ FB dependent mechanism that forms functional μVNs.

2. Materials and methods

2.1. Plasmids, lentivirus, and RT-PCR primers

pLV-hTERT-IRES-hygro was a gift from Tobias Meyer (Addgene plasmid # 85140; http://n2t.net/addgene:85140; RRID:Addgene_85140). lentiCRISPRv2 blast was a gift from Brett Stringer (Addgene plasmid # 98293; http://n2t.net/addgene:98293; RRID:Addgene_98293). lentiGuide-Hygro-mTagBFP2 was a gift from Kristen Brennand (Addgene plasmid # 99374; http://n2t.net/addgene:99374; RRID:Addgene_99374). pLX304 human Thy1 plasmid was from DNASU Plasmid Repository.

The following guide sequences were integrated into LentiCRISPRv2 blast for single gene knock out:

KO control [23]	GCACTACCAGAGCTAACTCA
IGFBP2	TCCTTCATACCCGACTTGAG
	GGCGATGACCACTCAGAAGG
	GGGCACTTGTGAGAAGCGCC
IGFBP7	TTCCATAGTGACGCCCCCCA
	GAGGCGGAAGGGTAAAGCCG
	GAGCAGGAGCAGCAGCCCAG
SPARC	CTTCTCAAACTCGCCAATGG

AGCCAGTCCCGCATGCGCAG
AGCCCTGCCTGATGAGACAG

Same guide sequences of KO control, IGFBP7 and SPARC were constructed into lentiGuide-Hygro-mTagBFP2 for double KO control and IGFBP7/SPARC double KO in ImFBs. 293 T cells were used for producing lentivirus. In short, the plasmids mentioned above were co-transfected with psPAX2, PMD. G using X-tremeGENE™ HP DNA Transfection Reagent (Sigma-Aldrich) for packaging into 293 T cells. The supernatant containing lentivirus was collected on day 2 and 3 post-transfection, followed by Lenti-X™ Concentrator (Takara Bio) mediated concentration. HUVECs, FBs, ImFBs, or Thy1− ImFBs were incubated overnight with the lentivirus in the presence of polybrene, 8 μg/ml. Infected cells were recovered for 24 h before selection by hygromycin or blasticidin. As for single gene KO in ImFBs, 3 types of KO lentiviruses were mixed and co-infected to ImFBs, and followed by blasticidin selection. For the IGFBP7/SPARC double KO in ImFBs, the IGFBP7 KO ImFBs were infected with mixtures of 3 types of SPARC KO lentiviruses. The BFP positive cells were sorted by fluorescence activated cell sorting (FACS). The KO efficiencies were detected by intracellular staining.

2.2. Cells, antibodies and reagents

HUVECs, ImHUVECs and HDMECs were cultured on uncoated T75 cell culture flasks in VascuLife VEGF Endothelial Medium (Lifeline Cell Technology). Lung FBs and ImFBs were cultured in FibroLife S2 Fibroblast Medium (supplied with 2% serum) or FibroLife Fibroblast Serum Free Medium (Lifeline Cell Technology). The medium was replenished every 2 days. Cells were detached and seeded into microfluidic devices after reaching 80% confluency. 293 T cells were cultured in DMEM medium containing 10% FBS without penicillin and streptomycin anti-biotics. Human IGFBP-2 antibody (R&D systems, 1:100), Anti-IGFBP7 antibody (Abcam, 1:60), Human SPARC PE-conjugated antibody (R&D systems, 1:100), hTERT antibody (Rockland, 1:200), and COL1A1 (E6A8E) Rabbit mAb (Cell Signaling Technology, 1:200) were used for IGFBP2, IGFBP7, SPARC, hTERT and Col1A1 staining, respectively. Anti-Fibroblast-PE, human (Miltenyi Biotec, 1:10), FITC anti-human CD90 (Thy1) antibody (Biolegend, 1:100), or APC anti-human CD90 (Thy1) antibody was used for fibroblast marker staining. Phorbol 12-myristate 13-acetate (PMA, 20 ng/ml) was from Sigma-Aldrich. Recombinant Human IGFBP2 (500 ng/ml), recombinant Human IGFBP7 (50 ng/ml), and recombinant Human SPARC (500 ng/ml) were purchased from Peprotech. Gelatin solution (Type B, 2%, Sigma-Aldrich) was diluted in PBS to 0.2% and incubated at 37 °C for 30 min for surface coating. Collagen I (Rat tail, Corning, 50 μg/ml) was used for surface coating following the protocol from the manufacture. Mitomycin C from Streptomyces caespitosus (Sigma-Aldrich) was diluted in complete FibroLife at 10 μg/ml or 20 μg/ml, and then incubated for 2.5 h followed with extensive washing before seeding into the microfluidic devices.

2.3. Microvascular network (μVN) formation

3D cell culture chips (AIM biotech) were utilized to generate *in vitro* μVNs. The microfluidic device contains three parallel channels: a central gel channel with two medium channels flanked along each side. Microposts are precisely spaced to separate fluidic channels and generate enough surface tension to confine the liquid gelling solution in the central channel before polymerization. The width of gel channel is 1.3 mm, gap between posts is 0.1 mm, height of channels is 0.25 mm, and the width of medium channels is 0.5 mm. ECs and FBs were seeded into the chip as previously described [4,24]. Briefly, ECs and FBs were concentrated in VascuLife containing thrombin (2 U/ml). The solution was then further mixed with fibrinogen (6 mg/ml) at a 1:1 ratio and quickly pipetted into the chip through the gel filling port with a final concentration of 7 million/ml for ECs and 1 million/ml for FBs. The device was placed in a humidified enclosure and allowed to polymerize at 37 °C for 15 min in a 5% CO_2 incubator, before VascuLife was introduced to the medium channels. After seeding, culture medium was changed on a daily basis in the device. The multi-culture microfluidic devices containing three parallel gel channels were fabricated as previously described [4,24]. Three hydrogel regions are each 0.8 mm wide × 1.3 mm long × 0.11 mm high, and separated by medium channels. ECs and FBs were seeded separately into the central gel channel and the two outer gel channels, respectively.

2.4. Microvascular network perfusion, imaging and analysis

To confirm the perfusability of μVNs, the culture medium in one side channel was aspirated, followed by injection of 20 μl of 10 μg/ml 70 kDa MW Texas Red dextran solution (Invitrogen). The process was then repeated for the other medium channel before imaging under a confocal microscope. Confocal images were acquired using an Olympus FLUO-VIEW FV1200 confocal laser scanning microscope with a 10× objective. Z-stack images were acquired with a 5 μm step size. Morphological parameters were analyzed and quantified using AngioTool [25]. The data of at least 16 ROIs from 3 biological replicates were used for analysis. The permeability of the μVN was measured as previously described [26], by quantifying the increase in fluorescence intensity of Texas Red-conjugated 70 kDa MW dextran in the matrix over 10 min. For the blocked opening analysis, if the FBs accumulated to the regions between microposts, especially aggregating at the interface between medium channel and gel channel, and ECs could not form an open structure towards medium channel, the microvessel opening would be counted as blocked. The blocked percentages were calculated by dividing the number of blocked openings by the total numbers of openings in each device. Cell accumulations between microposts were calculated using ImageJ (NIH, U.S.) by dividing the total fluorescence intensity of cells by the area of the region of interest (ROI) in the gap regions between microposts.

2.5. Flow cytometry

The expressions of Thy1 and anti-Fibroblast were tested by Flow cytometry (BD LSR-II). FBs were detached and stained with Anti-Fibroblast-PE, human (Miltenyi Biotec, 1:10), and FITC anti-human CD90 (Thy1) antibody (Biolegend, 1:100), or APC anti-human CD90 (Thy1) antibody (Biolegend, 1:100) on ice for 15 min. Cells were then washed twice with MACS buffer and were ready to be examined under flow cytometry. DAPI was used to

exclude dead cells. A BD FACSAria™ III Cell Sorter was used for cell sorting. To examine the expression of IGFBP2, IGFBP7, and SPARC, ImFBs were detached and then fixed by 4% paraformaldehyde (PFA) for 30 min. After being washed twice with PBS, the FBs were permeabilized with 0.1% Triton X-100, followed by blocking using 10% goat serum, and then stained with Human IGFBP-2 antibody (R&D systems, 1:100), Anti-IGFBP7 antibody (Abcam, 1:60), or Human SPARC PE-conjugated antibody (R&D systems, 1:100) on ice for 30 min. Cells were washed three times with PBS, stained with Alexa Fluor 633 Goat Anti-Mouse IgG1 (Invitrogen, 1:500, for IGFBP2), or Alexa Fluor 488 Goat Anti-Rabbit IgG H + L (Invitrogen, 1:1000, for IGFBP7) for 15 min, and rinsed three times with PBS before examination with Flow cytometry.

2.6. RNA isolation and RT-PCR

Total RNA was isolated using TRIzol reagent (Life Science). Reverse transcription was performed using High-Capacity RNA-to-cDNA™ Kit (Thermo Fisher Scientific). Quantitative Real-time RT-PCR (RT-PCR) using TB Green® Premix Ex Taq™ II (Tli RNase H Plus) (Takara), was performed with a 7900HT Fast Real-Time PCR System (Applied Biosystems). Glyceraldehyde 3-phosphate dehydrogenase (GAPDH) was used as the control housekeeping gene. Primers were synthesized by Genewiz. The following primers were used for RT-PCR detections:

GAPDH-F	ACCACAGTCCATGCCATCAC
GAPDH-R	TCCACCACCCTGTTGCTGTA
Thy1-F	GAAGGTCCTCTACTTATCCGCC
Thy1-R	TGATGCCCTCACACTTGACCAG
SPARC-F	TGCCTGATGAGACAGAGGTGGT
SPARC-R	CTTCGGTTTCCTCTGCACCATC
TGFBI-F	GGACATGCTCACTATCAACGGG
TGFBI-R	CTGTGGACACATCAGACTCTGC
IGFBP2-F	GGTATGAAGGAGCTGGCCGTGTTC
IGFBP2-R	CGCTGCCCGTTCAGAGACATCTTG
VEGFA-F	CGCAGCTACTGCCATCCAAT
VEGFA-R	GTGAGGTTTGATCCGCATAATCT
MMP14-F	CAACACTGCCTACGAGAGGA
MMP14-R	GTTCTACCTTCAGCTTCTGG
MMP2-F	GCGACAAGAAGTATGGCTTC
MMP2-R	TGCCAAGGTCAATGTCAGGA
COL1A1-F	GCTCGTGGAAATGATGGTGC
COL1A1-R	ACCAGGTTCACCGCTGTTAC
PCOLCE-F	CCAGACCCGTGTTCCTGTG
PCOLCE-R	CCCTCATCCGTCGTCATCC
IGFBP7-F	GAATCCCGACACCTGTCCTC
IGFBP7-R	TGGAGGTTTATAGCTCGGCAC
VEGFC-F	GCCAATCACACTTCCTGCCGAT

VEGFC-R	AGGTCTTGTTCGCTGCCTGACA
FGF2-F	AGCGGCTGTACTGCAAAAACGG
FGF2-R	CCTTTGATAGACACAACTCCTCTC

2.7. Intracellular immunofluorescence staining and molecular imaging

The intracellular immunofluorescence staining followed our previously published protocol [27,28]. In brief, ECs and FBs were loaded onto chambered cover glasses pretreated by plasma machine to increase adhesion, followed by 4% paraformaldehyde fixation for 30 min. After washing with 10 ml PBS, the ECs or FBs were permeabilized with 0.1% Triton X-100 and then blocked with 10% goat serum (Invitrogen). Subsequently, cells were stained with hTERT antibody (Rockland, 1:200) at 37 °C for 1 h. After washing with 10 ml PBS, these cells were stained with secondary antibody Alexa Fluor 647-conjugated goat anti-rabbit IgG (H + L) (Invitrogen, 1:500). Images were analyzed by ImageJ (NIH, U.S.).

2.8. Cell liberation from μVNs

The central gel channels in the microfluidic devices were manually cut out and incubated in 10% Liberase™ TH Research Grade (Sigma) diluted in DMEM on ice for 30 min. Samples were washed with MACS buffer and stained with Thy1 antibody as described above.

2.9. Treatment of ECs and FBs with PMA

For the Thy1 induction studies, ImHUVECs, Thy1+ ImFB, Thy1− ImFB, and FBs were cultured in 6-well plates and treated with Phorbol 12-myristate 13-acetate (PMA, Sigma-Aldrich, 20 ng/ml) at cell culture conditions for 48 or 96 h before the flow cytometry experiment [29]. DMSO was used as the vehicle control.

3. Results

3.1. μVNs made of immortalized ECs with FBs

In order to form μVNs in a robust manner from stable cell sources, we overexpressed hTERT to immortalize HUVECs and FBs that had been previously validated to form functional μVNs [30]. We verified hTERT expression in immortalized HUVECs (ImHUVECs) and immortalized FBs (ImFBs) using immunofluorescence staining and Western blot (Figure S1). The morphology of the μVNs made of ImHUVECs with ImFBs was comparable to that of the parental primary cells over 3 weeks (Fig. 1A–D). Next, we tested the capability of forming μVNs with the immortalized cells from later passages (passage 20, P20). ImHUVECs from P20 formed μVNs of good morphology that remained perfusable for three weeks but only with the support of earlier passage ImFBs (passage 5; Fig. 1 E–F, Figure S2). ImHUVECs formed μVNs in the presence of P20 ImFBs, but vessel area, junction density, vessel length, and perfusability were impaired (Fig. 1E–F).

3.2. Thy1+ FBs promote vasculogenesis but Thy1− FBs do not

Since ImFBs from later passages did not support the formation of functional μVNs, we characterized ImFBs from earlier and later passages by evaluating the expression of

fibroblast specific markers, anti-Fibroblast and Thy1 [31,32]. Nearly all ImFBs from P6 are positive for anti-Fibroblast antibody, but otherwise fall into nearly equal Thy1 positive (Thy1+) and Thy1 negative (Thy1−) subpopulations (Fig. 2A). P20 ImFBs remained positive for anti-Fibroblast antibody but few expressed Thy1 (Fig. 2A). Since trypsinization has been reported to cause a decrease in various surface proteins [33], we treated the cells with a gentle detachment reagent, TrypLE, but found no changes in Thy1 expression (Figure S3A). This indicates that the Thy1-subpopulation is not an artifact introduced by cell detaching processes. Next, to verify that the differences in Thy1 expression between these two subpopulations are not induced by immortalization or specific to this batch of FBs, we measured Thy1 and anti-Fibroblast expression in the ImFBs' parental FBs and primary lung FBs from 3 populations with different identifying lot numbers. Similar to ImFBs, all of these FBs contained both Thy1+ and Thy1-subpopulations (Figure S3 B–E). To investigate the functional difference between Thy1+ and Thy1− FBs, we sorted ImFBs from P6 based on Thy1 expression using fluorescence activated cell sorting (FACS) with over 95% purity (Figure S3F). The sorted cells were further expanded for experiments. Surprisingly, even though Thy1+ and Thy1− ImFBs exhibited similar morphology when cultured on 2D flasks (Fig. 2B), the Thy1− ImFBs failed to support perfusable μVN formation with ImHUVECs (Fig. 2C–D).

Next, we evaluated the μVN formation by human dermal microvascular endothelial cells (HDMEC) paired with Thy1+ or Thy1− ImFBs to determine if the inability of Thy1− ImFBs to support formation of functional μVNs was exclusive to co-culture with HUVECs. Consistently, Thy1+ ImFBs formed better μVNs than Thy1− ImFBs in terms of morphology and perfusability (Figure S4 A–E). To exclude the possibility that the defects in forming functional μVNs with Thy1− ImFBs were caused by immortalization, we compared the μVNs formed with Thy1+ and Thy1-parental primary FBs. Similarly, Thy1+ primary FBs formed μVNs with improved morphology compared to Thy1-primary FBs (Figure S4 F–G). Furthermore, to verify this phenotype was not specific to a particular batch of FBs, we repeated these experiments with a second batch of ImFBs (ImFB-2) made from a different lot number and observed the same results (Figure S4 H–J). Overall, these data indicate that the Thy1+ FBs promote vasculogenesis in comparison to Thy1− FBs.

3.3. The morphological defects in μVNs formed with Thy1− FBs are not caused by over-proliferation nor decreased Thy1 expression

Previous studies have found that Thy1 suppresses proliferation and promotes apoptosis in FBs [34]. Similarly, we observed that Thy1− ImFBs proliferate faster than Thy1+ ImFBs by detecting CFSE signals after culturing for 2 days (Fig. 3A). In addition, the overgrowth of FBs tended to correlate with regression of the μVNs (Fig. 3B). Thus, we hypothesized that the morphological defects in μVNs formed with Thy1− FBs may be due to FB over-proliferation. To test this, we forced Thy1− ImFBs senescence by pretreating them with mitomycin C [35], which suppresses cell proliferation by crosslinking double-stranded DNA. However, suppressing FB proliferation did not improve vasculature morphology (Fig. 3C). In parallel, we also reduced the initial seeding density of Thy1− ImFBs, but the defective vasculature morphology was not rescued (Figure S5). Thy1 is known to interact with integrin $\alpha_V\beta_3$ to regulate cell adhesion, migration, and mechanosensing [15,16]. To

further evaluate the function of Thy1 in vasculature formation, we overexpressed Thy1 in Thy1− ImFBs (Fig. 3D). However, the defective μVN morphology was not improved (Fig. 3E). This suggests that low Thy1 expression does not directly lead to the morphological defects in μVNs, and that Thy1 serves as a marker for some other phenotypic changes.

3.4. IGFBP2 expressed by Thy1+ FBs partially contributes to μVN formation

To explore the underlying mechanism, we used RT-PCR to evaluate the expression of several genes that are important for vascular lumen formation and angiogenesis. We found that Thy1+ FBs expressed more copies of certain factors than Thy1− FBs when cultured in 2D (Fig. 4 A). Among these factors, insulin-like growth factor-binding protein 2 (IGFBP2) has been found to promote angiogenesis [36,37]. We observed consistently higher expression of IGFBP2 in Thy1+ FBs compared to Thy1− FBs across different batches of FBs (Figure S6A). Addition of IGFBP2 to the culture medium during vasculogenesis partially rescued the defective morphology of μVNs formed with Thy1− FBs (Fig. 4B). Furthermore, we knocked out (KO) IGFBP2 in ImFBs (Fig. 4C) and sorted them into Thy1+ and Thy1− IGFBP2 KO FBs. We found that knocking out IGFBP2 in Thy1+ ImFBs impaired μVN formation (Fig. 4D). Adding IGFBP2 in the medium rescued the vascular defects in Thy1+ IGFBP2 KO ImFBs, but only partially rescued those defects in the Thy1− IGFBP2 KO ImFB group (Fig. 4D). This indicates that besides IGFBP2, there must be other factors that contribute to generating functional μVNs in Thy1+ FBs.

3.5. Thy1+ FBs express more IGFBP2, IGFBP7, and SPARC than Thy1− FBs to promote vasculogenesis

The μVNs are formed in 3D fibrin gels, where ECs and FBs may respond differently to the microenvironment as compared to 2D culture. Thus, we repeated the comparison of gene expression levels in Thy1+ and Thy1− ImFBs cultured in 3D fibrin gels. Remarkably, ImFBs cultured in 3D expressed distinct gene profiles (Figure S6B). Compared to Thy1− ImFBs, Thy1+ ImFBs in 3D expressed more of the vasculogenic and angiogenic factors, such as IGFBP7, SPARC, VEGFA, and VEGFC, but less collagen type I, alpha 1 (COL1A1, Fig. 5 A). Because VEGFC is primarily relevant in lymphatic EC function, rather than blood vascular, and because the endothelial cell growth culture medium we used for vasculogenic experiments is supplemented with VEGFA, we focused on IGFBP7 and SPARC, which are known to play important roles in vascular lumen formation [38]. We added IGFBP2, IGFBP7, and SPARC individually or in combination to the medium during μVN formation. Although adding IGFBP7 and SPARC together partially rescued morphological defects in the μVNs formed with Thy1− ImFBs, supplementing the combination of all three factors fully rescued those defects (Fig. 5B). Similarly, we verified the contribution of IGFBP7 and SPARC in μVN formation by knocking out individual or both genes in ImFBs (Figure S7).

3.6. Thy1− FBs physically block the microvessel openings, reducing vascular perfusability

Perfusability is another key feature for evaluating the functionality of μVNs. We observed that, while the perfusable μVNs have microvessel openings at the gap regions between microposts, those non-perfusable μVNs were closed at these locations (Fig. 6A). Although the combination of IGFBP2, IGFBP7, and SPARC rescued the morphological defects (vessel

area, junction density, and vessel length) in the μVNs formed with Thy1− ImFBs, the perfusability remained impaired. The μVNs formed with Thy1− ImFBs had fewer openings than the Thy1+ ImFB group, regardless of supplementation with IGFBP2, IGFBP7, and SPARC (Fig. 6B). We tracked the locations of the FBs and found that more Thy1− ImFBs accumulated in the gap regions between microposts during early vascularization (day 1–3) compared to Thy1+ ImFBs (Fig. 6C–D). The accumulation of FBs was associated with a reduction in ECs in Thy1− ImFB group than Thy1+ ImFB group starting from day 4 (Fig. 6E). Overcrowding by ImFBs at the gap regions between microposts appeared to be blocking the vascular openings (Fig. 6C). We quantified the percentage of FB-blocked regions in each device and found that Thy1− ImFBs blocked more gap regions than Thy1+ ImFBs (Fig. 6F). Since the RT-PCR results suggested an upregulation of COL1A1 in Thy1− FBs, we stained for COL1A1 in the μVNs. Indeed, fewer Thy1+ ImFBs expressed COL1A1 (Fig. 6G) and the amount of COL1A1 at the gap regions in the Thy1+ ImFB group was less than Thy1− ImFB group as quantified by immunofluorescent intensity (Fig. 6H). To determine if the presence of FBs and deposited collagen prevented microvessels from opening at the medium channel, we used a three-gel-channel microfluidic device that physically splits Thy1− ImFBs from ImHUVECs into separate side gel channels by medium channels [4,24]. ImHUVECs alone were seeded in the central gel channel (Fig. 6I), where they formed μVNs in the medium with IGFBP2, IGFBP7, and SPARC supplementation. The perfusability of the μVNs was improved with more unobstructed openings between microposts (Fig. 6J), supporting the hypothesis that FB crowding and/or collagen deposition may be partialy responsible for poor perfusability.

3.7. Thy1+ FBs gradually switch to Thy1− FBs after expansion in 2D and 3D

Next, we investigated how Thy1− FBs might become dominant in later passages. By testing Thy1 expression in the same FBs from different passages, we found that Thy1 expression decreased in FBs during expansion in 2D culture (Fig. 2A, Figure S8A). To confirm whether this phenomenon also occurs in 3D environments during *in vitro* vasculogenesis, we seeded ImHUVECs expressing GFP and Thy1+ or Thy1− ImFBs labeled with mCherry in microfluidic chips. On day 7, we collected the cells from the devices and tested Thy1 expression. Similar to 2D culture, we found that Thy1 expression decreased in the Thy1+ ImFBs, while the Thy1− ImFBs remained Thy1 negative compared to day 0 (Figure S8 B–C). This was also confirmed by utilizing RT-PCR to compare the Thy1 expression of ImFBs cultured in 3D fibrin gel on day 3 and day 7 (Figure S8D). Overall, our results indicate that Thy1 expression in FBs gradually decreased during expansion in both 2D and 3D cultures.

3.8. Thy1 expression is mostly maintained in serum-free medium

To make the ImFB a stable source to form functional μVNs, it appears essential to maintain the Thy1+ sub-population. As shown above, we discovered that Thy1+ FBs expressed more IGFBP2 than Thy1− FBs when cultured in 2D (Fig. 4B). Given that IGFBP2 has been shown to maintain the phenotypes of corneal FBs *in vitro* [39], we wondered whether supplementing IGFBP2 would maintain the Thy1+ subpopulation. We treated the primary FBs, Thy1+ ImFBs, and Thy1− ImFBs with IGFBP2 over 6 days, but found that supplementing IGFBP2 in the culture medium could not prevent the reduction of Thy1+

subpopulation (Figure S9A). It has also been shown that phorbol 12-myristate 13-acetate (PMA) can induce Thy1 expression in HUVECs [29]. To investigate whether PMA might be effective in inducing Thy1 expression, we next measured Thy1 expression in primary FBs, Thy1+ ImFBs, and Thy1− ImFBs treated with PMA for 48 h or 96 h. Unexpectedly, Thy1 expression was only slightly upregulated after being treated for 96 h (Figure S9B). Moreover, a previous study found that PMA inhibits the growth of human fibroblasts derived from embryonic skin [40]. Thus, PMA treatment is not an ideal method for maintaining Thy1+ FBs.

As mentioned above, Thy1− FBs proliferated more rapidly than Thy1+ FBs (Fig. 3A). Since the proliferation of FBs was mainly driven by FBS (Fig. 7A), we evaluated Thy1 expression in ImFBs cultured in serum-containing medium (2%) or serum-free medium. We found that the ImFBs cultured in serum-free medium maintained more Thy1 but were less proliferative than the ImFBs cultured in serum-containing medium (Fig. 7B–C). To overcome this limitation, we cultured the Thy1+ ImFBs on collagen I- or gelatin-coated surfaces and found that culturing on gelatin-coated surfaces in serum-free medium improved proliferation while preserving Thy1+ subpopulation (Fig. 7C–E). Furthermore, these Thy1+ ImFBs from later passages were able to support perfusable μVN formation (Fig. 7F).

4. Discussion

This study established ImHUVECs and ImFBs for μVN formation *in vitro* and reported that ImHUVECs are a stable source for vascularization, while the ImFBs from early passages support μVN formation but not later ones. Moreover, ImFBs are heterogeneous for Thy1 expression, include Thy1 positive (Thy1+) and Thy1 negative (Thy1−) subpopulations. We conclude that Thy1+ FBs form better μVNs in terms of morphology than Thy1− FBs, largely because of the higher expression of IGFBP2, IGFBP7, and SPARC. In addition, Thy1− FBs physically block the microvessel openings of μVNs, consequently forming less perfusable μVNs compared to Thy1+ FBs. Finally, culturing FBs on gelatin-coated surfaces in serum-free medium can maintain the majority of the Thy1+ subpopulation. Our study sheds light on the Thy1+ FB dependent mechanism to form perfusable μVNs with good morphology.

A stable cell source is essential for the reproducibility of both basic and clinical experimental research. Human primary cells derived from non-cancerous tissues have limited lifespans and eventually become senescent after a few passages when cultured *in vitro*. Exogenously expressing hTERT, which encodes the catalytic subunit of human telomerase, can prevent telomere shortening, overcome telomere-controlled senescence, and immortalize primary human cells [12]. This strategy has been used to immortalize various cell types, including ECs, FBs, epithelial cells, keratinocytes, and mesenchymal stem cells [12]. In terms of vasculogenesis *in vitro*, many studies have used HUVECs and lung FBs as stromal cells for vasculogenic studies *in vitro* [11,35,41–44]. Here, we overexpress hTERT in HUVECs and normal human lung FBs to establish ImHUVECs and ImFBs. These immortalized cells are proliferative and have been verified to form functional μVNs *in vitro*, thus providing stable cell sources for vascular research.

Although the immortalization strategy has shown promising applications, some studies have found underlying biological changes between immortalized cells and primary ones, such as metastases, immune system activation, and infection [45]. Immortalization of primary cells provides a relatively stable cell source for experimental purposes. All key discoveries from immortalized cells should be verified with diverse samples, different types of cells, or multiple models. In this paper, we also verified that Thy1+ FBs support μVN formation using both primary and immortalized cells (Fig. 2, Figure S4). Future work on developing other immortalized endothelial cells and stromal cells from diverse tissues would provide more choices for initial experimental studies.

Thy1+ and Thy1− FBs derived from lung tissues have been identified with distinct functions [19,20], such as proliferation [21], differentiation to myofibroblast, and correlation with fibrosis [15,22]. Similarly, we found that lung FBs have both Thy1+ and Thy1- subpopulations and that Thy1+ FBs promote μVN formation more robustly than Thy1− FBs. Moreover, overexpressing Thy1 in Thy1− FBs could not rescue the morphological defects in μVNs, indicating that such defects are not directly mediated by Thy1. Rather, Thy1 acts as a marker to distinguish these two subpopulations.

Thy1+ and Thy1− FBs derived from different tissue origins may have distinct phenotypes and functions. For example, Thy1-lung FBs derived from rats have higher α-SMA expression at baseline, indicating a myofibroblast phenotype [46]. In contrast, the Thy1+ and Thy1-lung FBs derived from normal human tissues in this study show no significant difference in morphology (Fig. 2B) or α-SMA expression (data not shown), although treating Thy1+ lung FBs with fibrogenic stimuli has been found to downregulate Thy1 expression *in vitro* [22]. It has been shown that only Thy1+ human myometrial and orbital FBs are capable of myofibroblast differentiation, while only Thy1-but not Thy1+ subsets can be differentiated to lipofibroblasts [32]. All these studies indicate the different phenotypes in Thy1 subsets of FBs derived from various origins, highlighting the importance of utilizing tissue-specific stromal cells of proper subsets for tissue engineering.

Recently, several studies induced FBs to become senescent [44] or be ablated [35] to improve μVN formation *in vitro*. Thy1 plays a crucial role in the control of cell growth by suppressing proliferation and promoting apoptosis and differentiation of dermal fibroblasts [34]. In addition, Thy1-lung FBs are more proliferative in response to fibrogenic stimuli [21]. We also observed that Thy1− FBs proliferate faster than Thy1+ FBs; however, forcing Thy1− FBs senescence cannot rescue the morphological defects in μVNs. It is possible that applying the FB-ablation strategy mentioned above [35] to the Thy1+ FBs could further improve morphology and prolong the lifespan of the μVNs.

By evaluating the expression of genes associated with angiogenesis and vasculogenesis, we found that Thy1+ FBs expressed more IGFBP2 than Thy1− FBs when cultured on 2D surfaces. IGFBP2 has been found to promote angiogenesis [36,37,47] and vasculogenic mimicry in glioma [48] through insulin-like growth factor I (IGF-I) dependent and independent pathways (interaction with $\alpha_V\beta_3/\alpha_V\beta_1$ integrin) [49,50]. In this study, we found that the addition of exogenous IGFBP2 could partially rescue the μVN morphological defects in the Thy1-group. We speculated that IGFBP2 expressed by Thy1+ FBs may

promote μVN formation through similar mechanisms for two reasons. First, IGF-I is one of the supplements in the culture medium used for μVN formation. Second, blocking $\alpha_V\beta_3/\alpha_V\beta_1$ integrins in vascular cells by adding the antagonist ATN-161 abolished μVN formation (data not shown). An indirect way to evaluate this hypothesis is to constitutively express active integrin [51] in ECs and test whether Thy1− FBs can form better μVNs with these ECs. These speculations are currently being investigated.

Previous studies have systematically explored fibroblast-derived matrix proteins for angiogenesis and lumen formation [38]. FB-derived collagen alpha-1 (COL1A1), procollagen C-endopeptidase enhancer 1 (PCOLCE), transforming growth factor-β–induced protein ig-h3 (TGFBI), insulin-like growth factor-binding protein 7 (IGFBP7), and secreted protein acidic and rich in cysteine (SPARC) were required for EC lumen formation [38]. In our studies, we found that Thy1− FBs cultured in 3D have lower expression levels of genes associated with lumen formation, especially SPARC and IGFBP7, than Thy1+ FBs. Furthermore, the addition of SPARC and IGFBP7 could improve the morphologically defective μVNs formed with Thy1− FBs. Our data are consistent with published results that IGFBP7 and SPARC are required for lumen formation [38]. However, in our microfluidic platform, only the addition of IGFBP2 in combination with IGFBP7 and SPARC could fully rescue the morphological defects in μVNs, indicating the importance of both angiogenesis and lumen formation during μVN formation. Previous studies have found that, although collagen 1 is required for lumen formation, the addition of collagen 1 alone cannot rescue lumen defects caused by knocking down lumen-formation associated genes in FBs [38]. This is consistent with our finding that Thy1− FBs express more COL1A1 than Thy1+ FBs, but form μVNs with poor morphology. Thy1− FBs also express more MMP14 than Thy1+ FBs at later time points, suggesting that unstable matrix remodeling may contribute to morphological defects in μVNs.

In addition to morphology, perfusability is a key factor for the functionality of μVNs. We found that the μVNs formed with Thy1− FBs were less perfusable, including those that were morphological rescued by the addition of IGFBP2, IGFBP7, and SPARC. To elucidate the mechanisms behind these data, we discovered that Thy1− FBs migrated to the gap regions between microposts in the microfluidic devices and physically block microvessel openings more frequently than Thy1+ FBs. The elevated COL1A1 expression in Thy1− FBs may further enhance such blocking effects. The recruitment of Thy1− FBs towards the gap regions between microposts may be regulated by both chemical and physical cues. The gap regions between microposts are connected to medium channels, where the growth factors and nutrients could attract FB migration. It has been shown that myofibroblast-like FBs are enriched and stabilized at the growth front (curved interface between 3D matrix and medium) by tensile force [52]. In our microfluidic device, the interface between the medium channel and gel channel provides this tensile force. Thus, both chemical and physical cues may contribute to the Thy1− FB accumulation at the gap regions between microposts. Another interesting result regarding FB accumulation is that the normalized FB accumulation at the gap regions between microposts are similar when comparing Thy1+ and Thy1− ImFBs on day 4. We have two possible explanations. First, Thy1+ FBs are switching to Thy1− ImFBs. As shown in Figure S8, Thy1+ ImFBs were switching to Thy1− ImFBs during vasculogenesis *in vitro*. Thus, the newly switched Thy1− FBs (previously

Thy1+) may increase the FB accumulation at the regions between microposts at the later stages in Thy1+ FB group. Second, the FBs that migrated out of the gel channel into the medium channels reside outside of the ROI and, therefore, are not included for accumulation analysis. In Fig. 6C, there are more ImFBs migrated into the medium channel in the Thy1− FB group than in the Thy1+ group even on day 3. Thus, the differences in FB accumulation are mild at the later stage. There may be other reasons as well, such as FB over-proliferation in the Thy1+ FB group, which require further evaluation.

5. Conclusions

In summary, we have established immortalized cell lines for vasculogenesis *in vitro*. Furthermore, our findings reveal that Thy1+ FBs promote perfusable μVN formation by expressing more IGFBP2, IGFBP7, and SPARC, as well as that they are less likely to produce blocking structures at microvessel openings than Thy1− FBs. Our studies have potentially important implications for organoid vascularization, tissue engineering, and the development of pathological models for basic and clinical research.

Supplementary Material

Refer to Web version on PubMed Central for supplementary material.

Acknowledgements

We thank the Flowcytometry Core facility at Koch Institute for Integrative Cancer Research at MIT for technical support. Z.W. is supported by the Ludwig Center Fund Post-Doctoral Research Fellowship and by the National Cancer Institute (U01 CA214381). S.E.S. is supported by a fellowship from the National Cancer Institute (K00CA212227). MC was supported by the MIT-POLITO grant (BIO-MODE-Compagnia di San Paolo) under the joint “Doctorate of Bioengineering and Medical-Surgical Sciences” of University of Turin and Politecnico di Torino. This work was supported by a National Cancer Institute Physical Sciences-Oncology Network award U01 CA214381.

Declaration of competing interest

RDK is the co-founder of and holds a significant financial interest in AIM Biotech, a company that produces microfluidic devices. RDK also receives research support from Amgen, Biogen, and W. L. Gore. DAB is a co-founder of and holds a significant financial interest in Xsphera Bio-sciences, and is a consultant for Qiagen/N of One. DAB has also received research funding from Novartis, Gilead Sciences, BMS, and Lilly Oncology.

Data availability

All data generated or analyzed during this study are included in this article (and its supplementary information files) and are available from the corresponding author upon request.

References

[1]. Auger FA, Gibot L, Lacroix D, The pivotal role of vascularization in tissue engineering, Annu. Rev. Biomed. Eng 15 (2013) 177–200. [PubMed: 23642245]

[2]. Geiger M, Fundamentals of Vascular Biology, Springer, 2019.

[3]. Zhang S, Wan Z, Kamm RD, Vascularized organoids on a chip: strategies for engineering organoids with functional vasculature, Lab Chip 21 (3) (2021) 473–488. [PubMed: 33480945]

[4]. Whisler JA, Chen MB, Kamm RD, Control of perfusable microvascular network morphology using a multiculture microfluidic system, Tissue Eng. C Methods 20 (2014) 543–552.

[5]. Moya ML, Hsu YH, Lee AP, Hughes CC, George SC, In vitro perfused human capillary networks, Tissue Eng. C Methods 19 (2013) 730–737.

[6]. Kim S, Lee H, Chung M, Jeon NL, Engineering of functional, perfusable 3D microvascular networks on a chip, Lab Chip 13 (2013) 1489–1500. [PubMed: 23440068]

[7]. Haase K, Kamm RD, Advances in on-chip vascularization, Regen. Med 12 (2017) 285–302. [PubMed: 28318376]

[8]. Rohringer S, Hofbauer P, Schneider KH, Husa AM, Feichtinger G, Peterbauer-Scherb A, et al. , Mechanisms of vasculogenesis in 3D fibrin matrices mediated by the interaction of adipose-derived stem cells and endothelial cells, Angiogenesis 17 (2014) 921–933. [PubMed: 25086616]

[9]. Haase K, Gillrie MR, Hajal C, Kamm RD, Pericytes contribute to dysfunction in a human 3D model of placental microvasculature through VEGF-ang-tie 2 signaling, Adv. Sci 6 (2019) 1900878.

[10]. Campisi M, Shin Y, Osaki T, Hajal C, Chiono V, Kamm RD, 3D self-organized microvascular model of the human blood-brain barrier with endothelial cells, pericytes and astrocytes, Biomaterials 180 (2018) 117–129. [PubMed: 30032046]

[11]. Mejías JC, Nelson MR, Liseth O, Roy K, A 96-well format microvascularized human lung-on-a-chip platform for microphysiological modeling of fibrotic diseases, Lab Chip 20 (2020) 3601–3611. [PubMed: 32990704]

[12]. Lee KM, Choi KH, Ouellette MM, Use of exogenous hTERT to immortalize primary human cells, Cytotechnology 45 (2004) 33–38. [PubMed: 19003241]

[13]. Reif AE, Allen JM, Immunological distinction of akr thymocytes, Nature 203 (1964) 886–887. [PubMed: 14204089]

[14]. Reif AE, Allen JM, The akr thymic antigen and its distribution in leukemias and nervous tissues, J. Exp. Med 120 (1964) 413–433. [PubMed: 14207060]

[15]. Rege TA, Hagood JS, Thy-1, a versatile modulator of signaling affecting cellular adhesion, proliferation, survival, and cytokine/growth factor responses, Biochim. Biophys. Acta 1763 (2006) 991–999. [PubMed: 16996153]

[16]. Hu P, Barker TH, Thy-1 in integrin mediated mechanotransduction, Front Cell Dev Biol 7 (2019) 22. [PubMed: 30859101]

[17]. Morris RJ, Thy-1, a pathfinder protein for the post-genomic era, Front Cell Dev Biol 6 (2018) 173. [PubMed: 30619853]

[18]. Saalbach A, Anderegg U, Thy-1: more than a marker for mesenchymal stromal cells, Faseb. J. : official publication of the Federation of American Societies for Experimental Biology 33 (2019) 6689–6696.

[19]. Phipps RP, Penney DP, Keng P, Quill H, Paxhia A, Derdak S, et al. , Characterization of two major populations of lung fibroblasts: distinguishing morphology and discordant display of Thy 1 and class II MHC, Am. J. Respir. Cell Mol. Biol 1 (1989) 65–74. [PubMed: 2576218]

[20]. Fries KM, Blieden T, Looney RJ, Sempowski GD, Silvera MR, Willis RA, et al. , Evidence of fibroblast heterogeneity and the role of fibroblast subpopulations in fibrosis, Clin. Immunol. Immunopathol 72 (1994) 283–292. [PubMed: 7914840]

[21]. Hagood JS, Mangalwadi A, Guo B, MacEwen MW, Salazar L, Fuller GM, Concordant and discordant interleukin-1-mediated signaling in lung fibroblast thy-1 subpopulations, Am. J. Respir. Cell Mol. Biol 26 (2002) 702–708. [PubMed: 12034569]

[22]. Hagood JS, Prabhakaran P, Kumbla P, Salazar L, MacEwen MW, Barker TH, et al. , Loss of fibroblast Thy-1 expression correlates with lung fibrogenesis, Am. J. Pathol 167 (2005) 365–379. [PubMed: 16049324]

[23]. Zhang Y, Shi J, Liu X, Feng L, Gong Z, Koppula P, et al. , BAP1 links metabolic regulation of ferroptosis to tumour suppression, Nat. Cell Biol 20 (2018) 1181–1192. [PubMed: 30202049]

[24]. Chen MB, Whisler JA, Frose J, Yu C, Shin Y, Kamm RD, On-chip human microvasculature assay for visualization and quantification of tumor cell extravasation dynamics, Nat. Protoc 12 (2017) 865–880. [PubMed: 28358393]

[25]. Zudaire E, Gambardella L, Kurcz C, Vermeren S, A computational tool for quantitative analysis of vascular networks, PloS One 6 (2011), e27385. [PubMed: 22110636]

[26]. Offeddu GS, Haase K, Gillrie MR, Li R, Morozova O, Hickman D, et al. , An on-chip model of protein paracellular and transcellular permeability in the microcirculation, Biomaterials 212 (2019) 115–125. [PubMed: 31112823]

[27]. Wan Z, Chen X, Chen H, Ji Q, Chen Y, Wang J, et al. , The activation of IgM- or isotype-switched IgG- and IgE-BCR exhibits distinct mechanical force sensitivity and threshold, eLife 4 (2015).

[28]. Wan Z, Xu C, Chen X, Xie H, Li Z, Wang J, et al. , PI(4,5)P2 determines the threshold of mechanical force-induced B cell activation, J. Cell Biol 217 (7) (2018) 2565–2582. [PubMed: 29685902]

[29]. Wen HC, Huo YN, Chou CM, Lee WS, PMA inhibits endothelial cell migration through activating the PKC-delta/Syk/NF-kappaB-mediated up-regulation of Thy-1, Sci. Rep 8 (2018) 16247. [PubMed: 30389973]

[30]. Hajal C, Ibrahim L, Serrano JC, Offeddu GS, Kamm RD, The effects of luminal and trans-endothelial fluid flows on the extravasation and tissue invasion of tumor cells in a 3D in vitro microvascular platform, Biomaterials 265 (2021) 120470. [PubMed: 33190735]

[31]. Kahounova Z, Kurfurstova D, Bouchal J, Kharaishvili G, Navratil J, Remsik J, et al. , The fibroblast surface markers FAP, anti-fibroblast, and FSP are expressed by cells of epithelial origin and may be altered during epithelial-to-mesenchymal transition, Cytometry Part A : the journal of the International Society for Analytical Cytology 93 (2018) 941–951. [PubMed: 28383825]

[32]. Koumas L, Smith TJ, Feldon S, Blumberg N, Phipps RP, Thy-1 expression in human fibroblast subsets defines myofibroblastic or lipofibroblastic phenotypes, Am. J. Pathol 163 (2003) 1291–1300. [PubMed: 14507638]

[33]. Tsuji K, Ojima M, Otabe K, Horie M, Koga H, Sekiya I, et al. , Effects of different cell-detaching methods on the viability and cell surface antigen expression of synovial mesenchymal stem cells, Cell Transplant. 26 (2017) 1089–1102. [PubMed: 28139195]

[34]. Schmidt M, Gutknecht D, Simon JC, Schulz JN, Eckes B, Anderegg U, et al. , Controlling the balance of fibroblast proliferation and differentiation: impact of thy-1, J. Invest. Dermatol 135 (2015) 1893–1902. [PubMed: 25739049]

[35]. Song HHG, Lammers A, Sundaram S, Rubio L, Chen AX, Li L, et al. , Transient support from fibroblasts is sufficient to drive functional vascularization in engineered tissues, Adv. Funct. Mater (2020) 2003777. [PubMed: 33613149]

[36]. Azar WJ, Azar SH, Higgins S, Hu JF, Hoffman AR, Newgreen DF, et al. , IGFBP-2 enhances VEGF gene promoter activity and consequent promotion of angiogenesis by neuroblastoma cells, Endocrinology 152 (2011) 3332–3342. [PubMed: 21750048]

[37]. Das SK, Bhutia SK, Azab B, Kegelman TP, Peachy L, Santhekadur PK, et al. , MDA-9/syntenin and IGFBP-2 promote angiogenesis in human melanoma, Canc. Res 73 (2013) 844–854.

[38]. Newman AC, Nakatsu MN, Chou W, Gershon PD, Hughes CC, The requirement for fibroblasts in angiogenesis: fibroblast-derived matrix proteins are essential for endothelial cell lumen formation, Mol. Biol. Cell 22 (2011) 3791–3800. [PubMed: 21865599]

[39]. Park SH, Kim KW, Kim JC, The role of insulin-like growth factor binding protein 2 (IGFBP2) in the regulation of corneal fibroblast differentiation, Invest. Ophthalmol. Vis. Sci 56 (2015) 7293–7302. [PubMed: 26559475]

[40]. Bi N, Mamrack MD, PMA inhibits the growth of human fibroblasts after the induction of immediate-early genes, Exp. Cell Res 212 (1994) 105–112. [PubMed: 8174632]

[41]. Haase K, Offeddu GS, Gillrie MR, Kamm RD, Endothelial regulation of drug transport in a 3D vascularized tumor model, Adv. Funct. Mater (2020) 2002444. [PubMed: 33692661]

[42]. Zeinali S, Bichsel CA, Hobi N, Funke M, Marti TM, Schmid RA, et al. , Human microvasculature-on-a chip: anti-neovasculogenic effect of nintedanib in vitro, Angiogenesis 21 (2018) 861–871. [PubMed: 29967964]

[43]. Kim J, Chung M, Kim S, Jo DH, Kim JH, Jeon NL, Engineering of a biomimetic pericyte-covered 3D microvascular network, PloS One 10 (2015), e0133880. [PubMed: 26204526]

[44]. Xiao Y, Liu C, Chen Z, Blatchley MR, Kim D, Zhou J, et al. , Senescent cells with augmented cytokine production for microvascular bioengineering and tissue repairs, Adv Biosyst 3 (2019).

[45]. Lidington EA, Moyes DL, McCormack AM, Rose ML, A comparison of primary endothelial cells and endothelial cell lines for studies of immune interactions, Transpl. Immunol 7 (1999) 239–246. [PubMed: 10638837]

[46]. Zhou Y, Hagood JS, Murphy-Ullrich JE, Thy-1 expression regulates the ability of rat lung fibroblasts to activate transforming growth factor-beta in response to fibrogenic stimuli, Am. J. Pathol 165 (2004) 659–669. [PubMed: 15277239]

[47]. Slater T, Haywood NJ, Matthews C, Cheema H, Wheatcroft SB, Insulin-like growth factor binding proteins and angiogenesis: from cancer to cardiovascular disease, Cytokine Growth Factor Rev. 46 (2019) 28–35. [PubMed: 30954375]

[48]. Liu Y, Li F, Yang YT, Xu XD, Chen JS, Chen TL, et al. , IGFBP2 promotes vasculogenic mimicry formation via regulating CD144 and MMP2 expression in glioma, Oncogene 38 (2019) 1815–1831. [PubMed: 30368528]

[49]. Bid HK, Zhan J, Phelps DA, Kurmasheva RT, Houghton PJ, Potent inhibition of angiogenesis by the IGF-1 receptor-targeting antibody SCH717454 is reversed by IGF-2, Mol. Canc. Therapeut 11 (2012) 649–659.

[50]. Pereira JJ, Meyer T, Docherty SE, Reid HH, Marshall J, Thompson EW, et al. , Bimolecular interaction of insulin-like growth factor (IGF) binding protein-2 with alphavbeta3 negatively modulates IGF-I-mediated migration and tumor growth, Canc. Res 64 (2004) 977–984.

[51]. Van Agthoven JF, Xiong JP, Alonso JL, Rui X, Adair BD, Goodman SL, et al. , Structural basis for pure antagonism of integrin alphaVbeta3 by a high-affinity form of fibronectin, Nat. Struct. Mol. Biol 21 (2014) 383–388. [PubMed: 24658351]

[52]. Kollmannsberger P, Bidan CM, Dunlop JWC, Fratzl P, Vogel V, Tensile forces drive a reversible fibroblast-to-myofibroblast transition during tissue growth in engineered clefts, Sci Adv 4 (2018), eaao4881. [PubMed: 29349300]

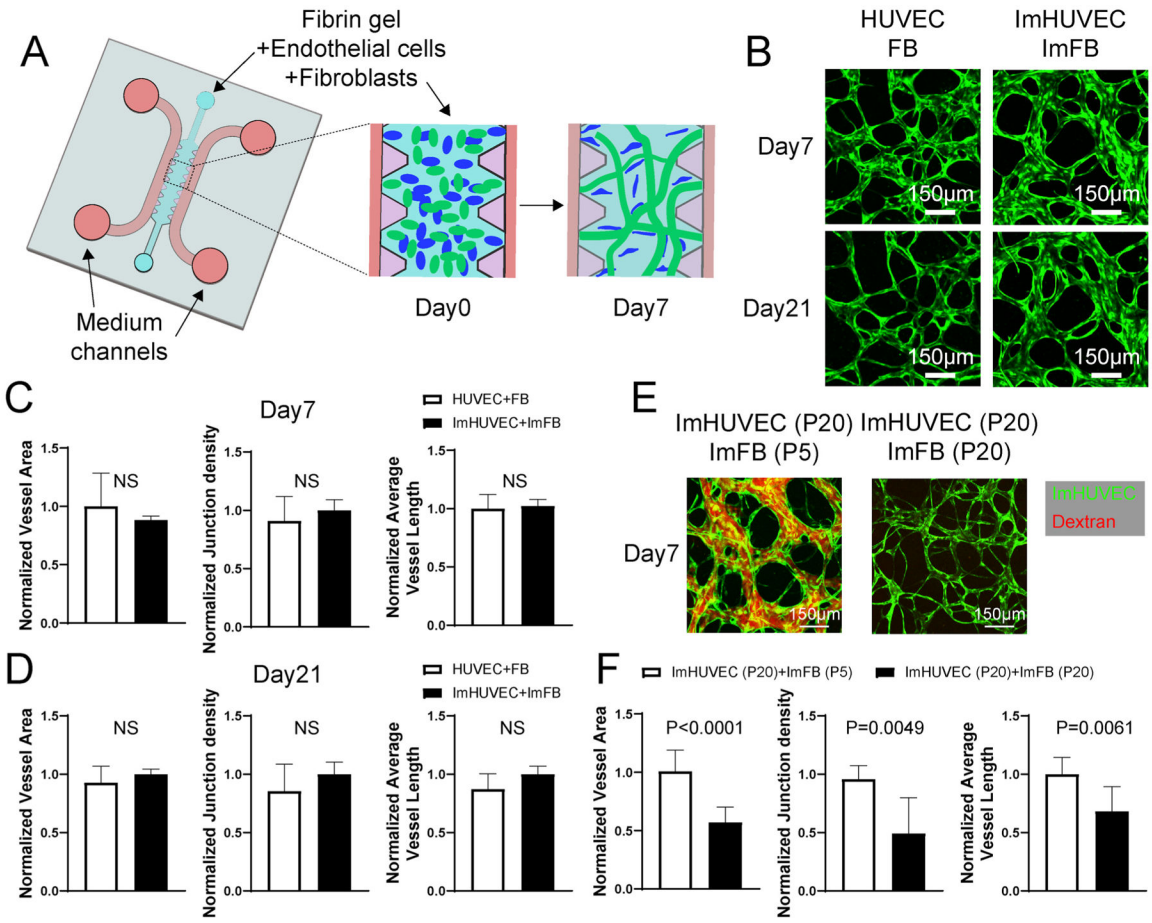

Fig. 1.

ImHUVECs form better μVNs with ImFBs from earlier passages than with ImFBs from later passages. (A) Schematic diagram of the AIMchip used to generate microvascular networks (μVNs) encapsulated in fibrin gel. Endothelial cells (ECs) and fibroblasts (FBs) mixtures are seeded on day 0 and form μVNs by day 7. (B) Representative images of μVNs made of parental HUVECs and FBs, as well as immortalized HUVECs (ImHUVECs) and immortalized FBs (ImFBs) on day 7 and day 21. Green: ECs. **(C–D)** Normalized vessel area (left), junction density (middle), and average vessel length (right) analyses of μVNs made of HUVECs with FBs or ImHUVECs with ImFBs on day 7 **(C)** and day 21 **(D)**. (E) Representative images of μVNs made of ImHUVECs (green) from passage 20 (P20) with ImFBs from passage 5 (P5) or ImFBs from P20. μVNs are perfused with Texas Red dextran (red). (F) Normalized vessel area (left), junction density (middle), and average vessel length (right) analyses of μVNs made of ImHUVECs (P20) with ImFBs (P5) or ImFBs (P20). Bars represent mean ± SD. Two-tailed *t* tests were performed for the statistical comparisons. Scale bar is 150 μm.

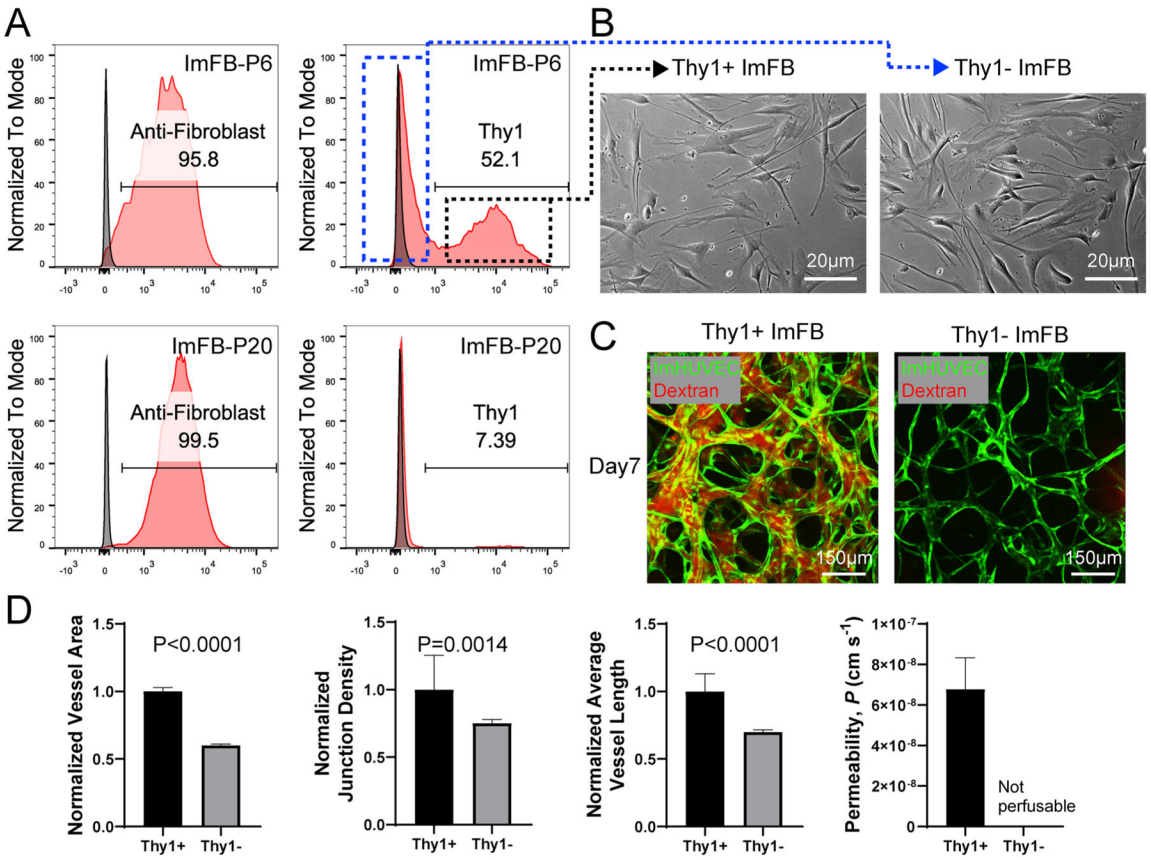

Fig. 2.

Thy1+ FBs promote vasculogenesis compared to Thy1− FBs. (A) Representative histograms showing expression of anti-Fibroblast and Thy1 in ImFBs from P6 (top) and P20 (bottom). Dotted rectangle indicates Thy1-subpopulation (blue) and Thy1+ subpopulation (black) for cell sorting. (B) Representative images of Thy1+and Thy1− ImFB monolayers. Scale bar is 20 μm. (C) Confocal images of μVNs made of ImHUVECs with Thy1+ or Thy1− ImFBs. Scale bar is 150 μm. (D) Normalized vessel area (far left), junction density (left), average vessel length (right) and permeability (far right) analyses of μVNs made of ImHUVECs with Thy1+ or Thy1− ImFBs. Bars represent mean ± SD. Two-tailed *t* tests were performed for the statistical comparisons.

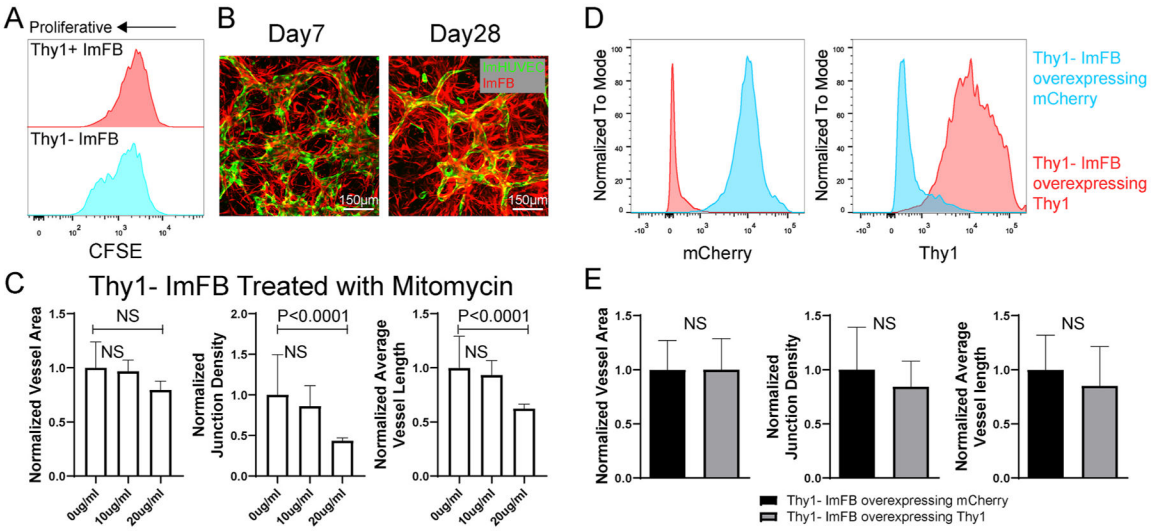

Fig. 3.

Neither over-proliferation nor decreased Thy1 causes defective μVN formation with Thy1− FBs. (A) Comparison of proliferation between Thy1+ and Thy1− ImFBs by monitoring CFSE. (B) Representative images of μVNs made of ImHUVECs with ImFBs on day 7 and day 28 (FB over-proliferation). Green, ImHUVECs. Red, ImFBs. Scale bar is 150 μm. (C) Statistical analysis of normalized vessel area (left), junction density (middle), and average vessel length (right) of μVNs formed with Thy1− ImFBs treated with 0, 10 or 20 μg/ml mitomycin C for 2.5 h before seeding. (D) Flowcytometry measurements of mCherry (left) and Thy1 (right) in Thy1− ImFBs overexpressing mCherry as control (blue), or Thy1− ImFBs overexpressing Thy1 (red). (E) Statistical analysis of normalized vessel area (left), junction density (middle), and average vessel length (right) of μVNs formed with Thy1− ImFBs overexpressing mCherry or Thy1. Bars represent mean ± SD. Two-tailed *t* tests were performed for the statistical comparisons.

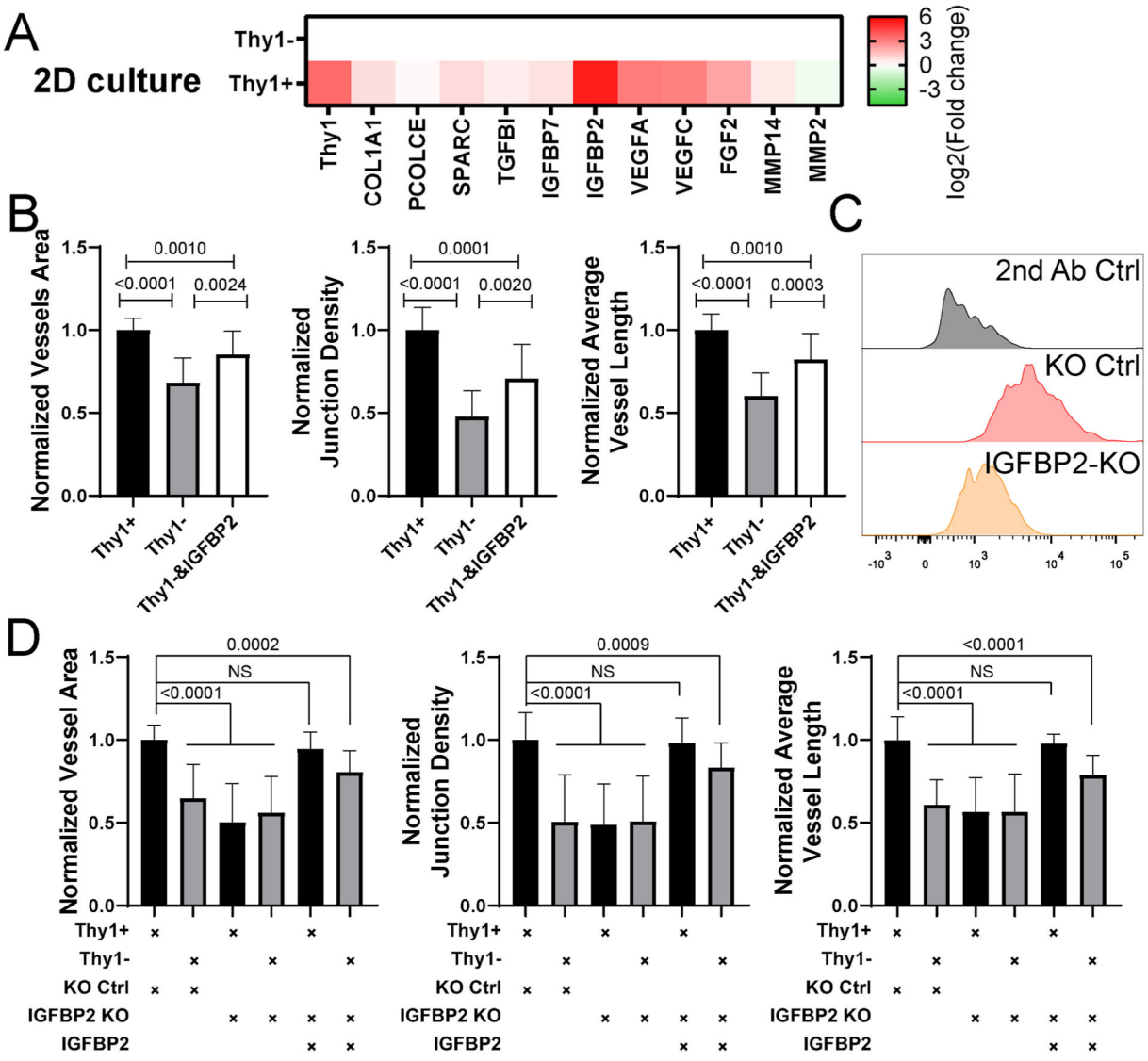

Fig. 4.

IGFBP2 partially rescues the morphological defects in μVNs formed with Thy1− FBs. (A) Heatmap of RT-PCR results of Thy1+ and Thy1− ImFB 2D monolayers. Fold change was relative to Thy1− ImFBs. (B) Normalized vessel area (left), junction density (middle), and average vessel length (right) analyses of μVNs formed with Thy1+, Thy1−, or Thy1− ImFBs supplemented with IGFBP2. (C) Representative histograms showing expression of IGFBP2 in knock out (KO) control ImFBs and IGFBP2 KO ImFBs. (D) Normalized vessel area (left), junction density (middle), and average vessel length (right) analyses of μVNs formed with Thy1+ KO control ImFBs, Thy1− KO control ImFBs, Thy1+ IGFBP2 KO ImFBs or Thy1− IGFBP2 KO ImFBs supplemented with or without IGFBP2. Bars represent mean ± SD. Two-tailed *t* tests were performed for the statistical comparisons.

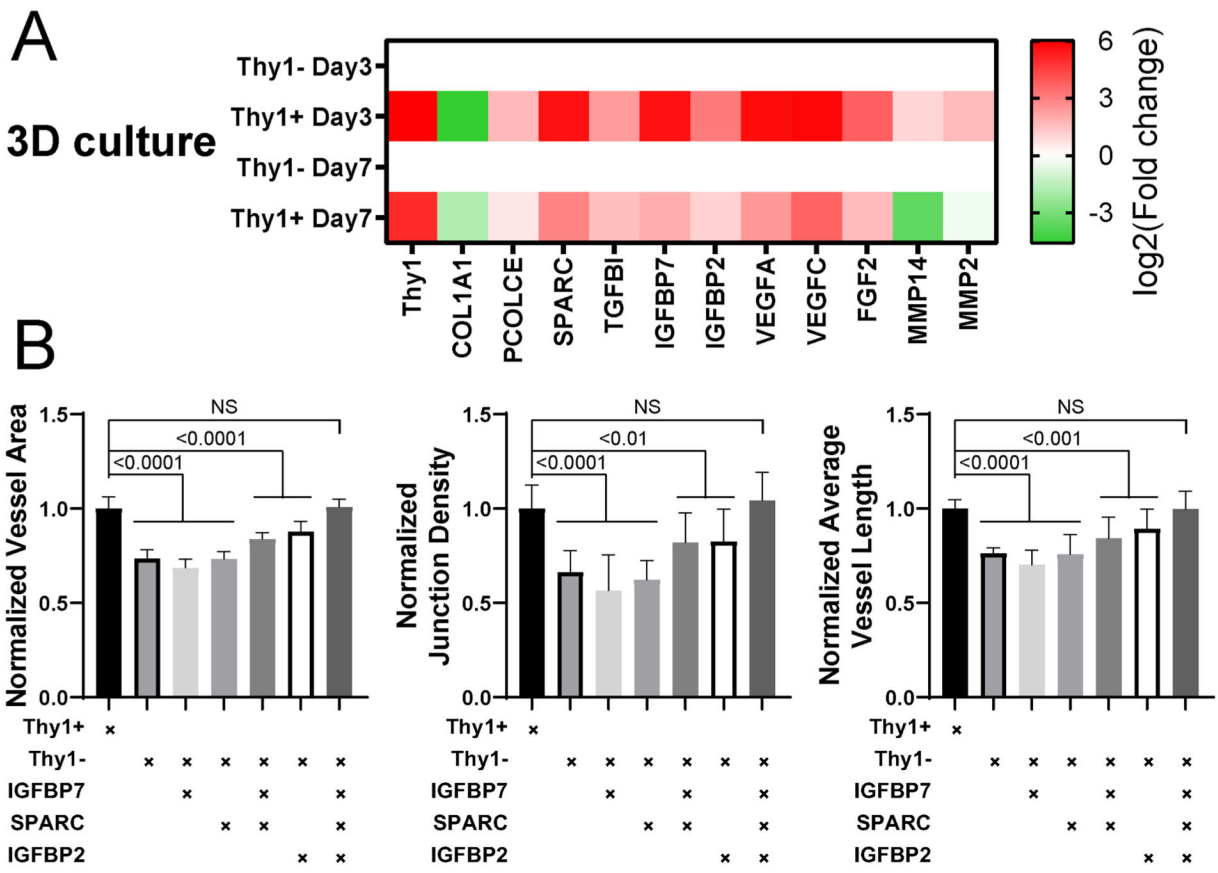

Fig. 5.

Combination of IGFBP2, IGFBP7, and SPARC rescues the morphological defects in μVNs formed with Thy1− FBs. (A) Heatmap of RT-PCR results of Thy1+ and Thy1− ImFBs cultured in 3D fibrin gel for 3 days or 7 days. Fold change was relative to Thy1− ImFBs. (B) Normalized vessel area (left), junction density (middle), and average vessel length (right) analyses of μVNs formed with Thy1+, Thy1−, and Thy1− ImFBs supplemented with or without IGFBP7, SPARC, and/or IGFBP2. Bars represent mean ± SD. Two-tailed *t* tests were performed for the statistical comparisons.

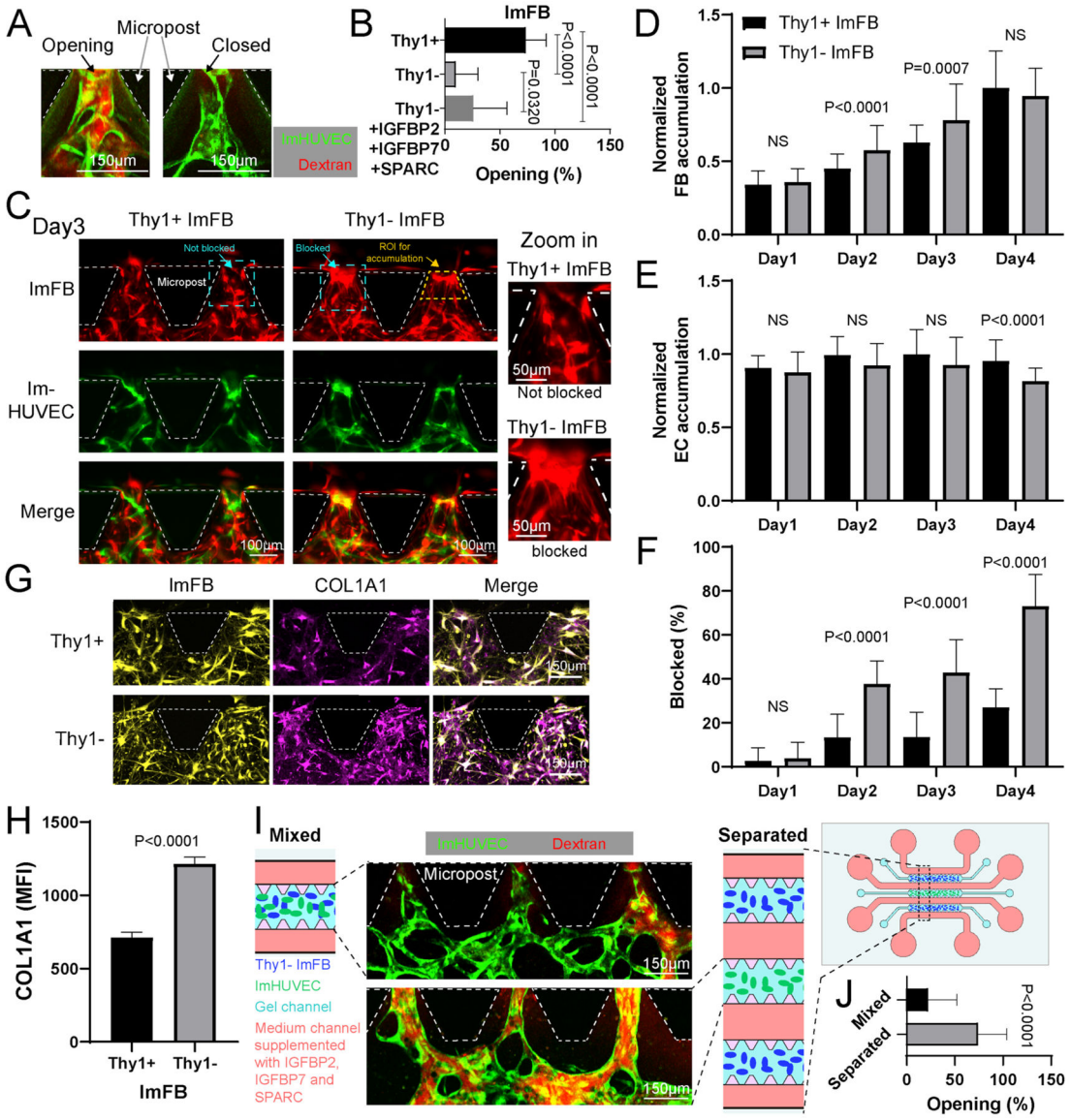

Fig. 6.

Thy1− FBs block microvessel openings and reduce μVN perfusability. (A) Representative confocal images of open and closed microvessels at the gap regions between microposts. Green, ImHUVECs. Red, dextran. (B) Percentage of microvessel openings in each region of interest. (C) Representative images of μVNs formed with Thy1+ or Thy1− ImFBs at the gap regions between microposts on day 3. Magnified images of cyan dashed squares are on the right to show the location of ImFBs forming not blocked or blocked structures. The yellow dashed line highlights the region of interest (ROI) for accumulation analysis in figure D and E. **(D, E)** Statistical analysis of ImFB **(D)** and ImHUVEC **(E)** accumulation at the gap regions between microposts from day 1 to day 4. (F) Percentage of blocked openings at the gap regions between microposts from day 1 to day 4. (G) Representative images of ImFBs and alpha-1 type 1 collagen (COL1A1) immunofluorescent staining in μVNs at the gap regions between microposts on day 3. (H) Statistical quantification of the mean fluorescent

intensity (MFI) of COL1A1 at the gap regions between microposts on day 3. (I) Schematic diagram and representative images of the μVNs made of ImHUVECs with Thy1− ImFBs seeded in the single gel channel device (Mixed) or the 3-gel channel devices (Separated). Cells were cultured with Vasculife medium supplemented with IGFBP2, IGFBP7, and SPARC. (J) Statistical quantification of the percentage of microvessel openings at the gap region between microposts in mixed or separated devices. Bars represent mean ± SD. Two-tailed *t* tests were performed for the statistical comparisons.

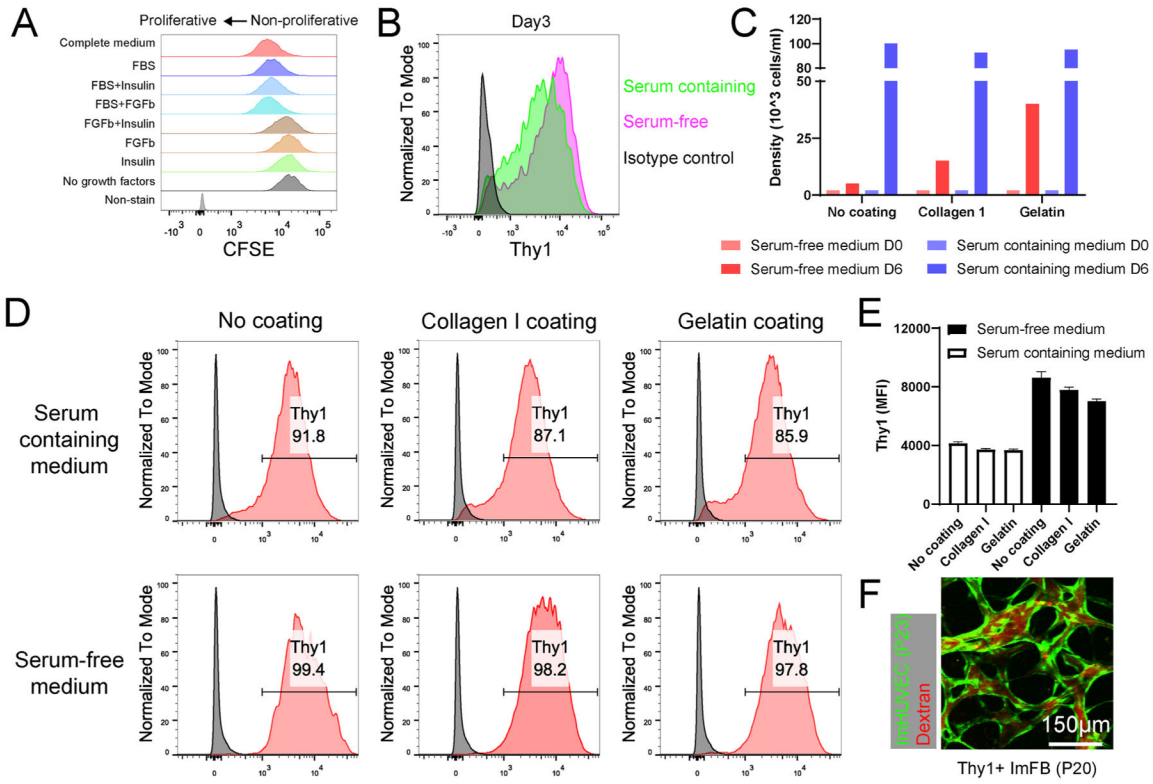

Fig. 7.

FBs maintain Thy1 expression in serum-free culture medium. (A) Representative histograms showing the proliferation of ImFBs cultured in the FB medium (Fibrolife) supplemented with different growth factors. ImFBs were stained with CFSE as proliferation indicator. (B) Representative histograms showing the Thy1 expression in ImFBs cultured in serum-containing medium or serum-free medium for 3 days. (C) Statistical quantification of Thy1+ ImFB cell density cultured in serum-containing medium or serum-free medium on day 0 (D0) and day 6 (D6). **(D, E)** Representative histograms **(D)** and statistical analysis **(E)** showing the Thy1 expression in ImFBs cultured in serum-containing medium or serum-free medium on collagen I- or gelatin-coated surfaces. (F) Representative images of μVNs made of ImHUVECs (P23, green) with Thy1+ ImFB (P20). μVNs are perfused with Texas Red dextran (red). Scale bar is 150 μm.